Journal of Nuclear Materials 415 (2011) S463–S466

Contents lists available at ScienceDirect

Journal of Nuclear Materials

journal homepage: www.elsevier.com/locate/jnucmat

Estimate of convective radial transport due to SOL turbulence as measured by GPI in Alcator C-Mod

S.J. Zweben [a,*], J.L. Terry [b], B. LaBombard [b], M. Agostini [c], M. Greenwald [b], O. Grulke [d], J.W. Hughes [b], D.A. D'Ippolito [e], S.I. Krasheninnikov [f], J.R. Myra [e], D.A. Russell [e], D.P. Stotler [a], M. Umansky [g]

[a] PPPL, P.O. Box 451, Princeton, NJ 08540, USA
[b] PSFC, MIT, Cambridge, MA 02139, USA
[c] Consorzio RFX, Padova, Italy
[d] IPP, Garching, Germany
[e] Lodestar Research, Boulder, CO 80301, USA
[f] UCSD, San Diego, CA 92093, USA
[g] LLNL, Livermore, CA 94550, USA

ARTICLE INFO

Article history:
Available online 22 August 2010

ABSTRACT

The convective radial transport effects of SOL turbulence have been estimated using recent turbulence data from the gas puff imaging (GPI) camera diagnostic on Alcator C-Mod. The average radial turbulence speed within the region 1–2 cm outside the separatrix near the outer was calculated by a 2-D cross-correlation technique to be $V_r \sim 0.2$–0.3 km/s. Assuming this to be the local convective plasma velocity, the density SOL width λ_n was evaluated using a simple convective model to be $\lambda_n \sim 4$–7 cm, which is ~2–3 times higher than that measured using a Langmuir probe. This convective velocity was also ~2–3 times lower than the velocities estimated from analytic blob models, but showed a similar scaling with plasma current at constant q_{95}. The measured blob speeds were lower than both the convective speeds and the analytic blob model speeds.

1. Introduction

The width of the tokamak scrape-off-layer (SOL) and its relationship to SOL turbulence has been studied for almost 30 years [1]. Traditionally, most SOL models assumed an *ad hoc* turbulent diffusivity or heat conduction in order to match the observed particle and heat SOL widths [2]. However, recent observations of intermittent convective transport in the SOL [2,3] and the development of analytic blob models [4] have shifted attention to the convective contributions to SOL transport.

Several recent papers have discussed the observed relationship between convective transport and the observed SOL width. For example, SOL profile measurements in C-Mod showed clear deviations from a diffusive flux-gradient relationship [5], and radial transport due to intermittency contributed ~50% of the SOL particle flux in DIII-D [6]. SOL profiles in JET and TCV have been modeled by a convective particle flow [7], and UEDGE modeling has been done using convection instead of diffusion [8]. Recently direct comparisons have been made between SOL widths and the results from 2-D SOL turbulence codes ESEL (for JET) [7], and SOLT (for NSTX) [9].

* Corresponding author.
E-mail address: szweben@pppl.gov (S.J. Zweben).

0022-3115/$ - see front matter © 2010 Elsevier B.V. All rights reserved.
doi:10.1016/j.jnucmat.2010.08.018

2. Cross-correlation measurement of convective velocity

The GPI diagnostic measures the D_α light emission and its fluctuations in the SOL, and so cannot directly measure the radial convective speed $V_r = \Gamma_\perp/n = \langle\delta n\, \delta V_r\rangle/n$, where $\Gamma_\perp$ is the radial particle flux, δn is the fluctuating density and δV_r is the fluctuating radial plasma velocity. However, if the D_α light emission is well correlated with the density fluctuations (as expected), then the local $\delta n/n$ and δV_r can (in principle) be evaluated from the GPI data.

Estimates of turbulence velocity from cross-correlations of the gas puff imaging (GPI) data on C-Mod have been described previously [10,11]. The GPI measurements described in the present paper were made using a Phantom 7.3 camera operated at 250,000 frames/s with a 64 × 64 pixel resolution, which are the same for the PSI-5 camera used previously. However, the present camera recorded 30,000 frames/shot, whereas the previous camera recorded only 300 frames/shot; thus the new system produces a much a larger set of data than previously. Typical turbulence size scales in the region ρ (i.e. distance outside separatrix) ~ 1–2 cm (the mid-to-far SOL, not including the limiter shadow) are $L_r \sim L_p \sim 0.7$–1.0 cm (FWHM), typical autocorrelation times are $\tau_{auto} \sim 10$–30 µs (to 50% correlation), and typical GPI light fluctuation levels are $dI/I \sim 0.2$–0.5, all similar to previous GPI measurements in C-Mod.

The velocity from the turbulence cross-correlations would clearly be the exact radial convective velocity if the plasma was moving outward at a constant speed everywhere in the SOL. If the local velocity had a low fluctuation level around some non-zero mean, then this velocity should still be a good approximation to the average convective velocity. However, if the velocity has a near-zero mean value, e.g. if the SOL transport was diffusive, then this method would not result in a useful convective velocity. In this section we assume that the convective velocity can be calculated from cross-correlation analysis, and in Section 4 we estimate the SOL width from this velocity. In Section 5 we describe an alternate way to calculate the convective SOL velocity and transport assuming the velocity fluctuations are large, i.e. blob-like.

The radial convective velocity of the turbulence was calculated by the cross-correlation method as follows: (a) for each point in each image, a delayed-time cross-correlation coefficient was calculated for all nearby points using a fixed delay time (less than τ_{auto}), and the results were then averaged over 10 ms, (b) the peak of the cross-correlation coefficient was located in 2-D, and then the radial velocity of the turbulence was calculated from the radial displacement of this peak from the initial pixel, divided by the chosen delay time, (c) these results were averaged over the central 4.5 cm of the poloidal range of these images for each radial column of pixels. The results were independent of the chosen cross-correlation delay time over 4–20 μs, and a similar result is obtained by fitting the peak correlation location vs. delay time. Note that this process averages over *all* the turbulence, including intermittent blobs and Gaussian components.

Typical results from this radial velocity analysis are shown in Fig. 1 for a normal Ohmic C-Mod deuterium discharge with B = 5.4 T, I = 1.0 MA, line-averaged $n_e = 1.3 \times 10^{20}$ m^{-3}, elongation κ = 1.6, and q_{95} = 3.7. Each point in Fig. 1 represents the analysis of one 10 ms period from one of two similar shots. The radial velocities vary significantly with radius, but for the region $\rho \sim$ 1–2 cm the result is an outward speed of $V_r \sim$ 0.2 km/s (i.e. ~1 mm/frame). The radial velocity decreases to near zero at $\rho \sim$ 0.5 cm, perhaps because the turbulence motion is diffusive there. The poloidal velocities in $\rho \sim$ 1–2 cm (not shown) are typically $V_p \sim$ 0.2–0.7 km/s, and decrease with radius.

Fig. 2a shows the average radial velocity integrated over $\rho \sim$ 1–2 cm for a set of 11 shots in a moderate density Ohmic current scan at fixed $q(a) \sim$ 3.7, which includes the data of Fig. 2 at I = 1.0 MA. These plasmas (#1090813005–020) had I = 0.4–1.1 MA, B = 2.3–6.0 T, $\langle n \rangle = 0.8–1.6 \times 10^{20}$ m^{-3}, $n(\rho = 1.5$ cm$) \sim 1 \times 10^{19}$ m^{-3}, and $T_e(\rho = 1.5$ cm$) \sim$ 20 eV. The estimated radial velocities decreased

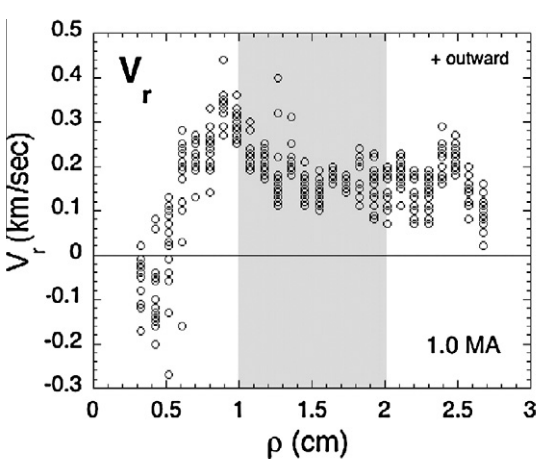

Fig. 1. Radial distribution of convective velocities obtained from cross-correlation analysis for the I = 1.0 MA discharges (#1090813007, 1090813008). Each point corresponds to a single 10 ms period in one of these discharges during the GPI gas puff (0.95–1.01 s). The shadowed region within ρ = 1–2 cm is the range of interest for the SOL analysis.

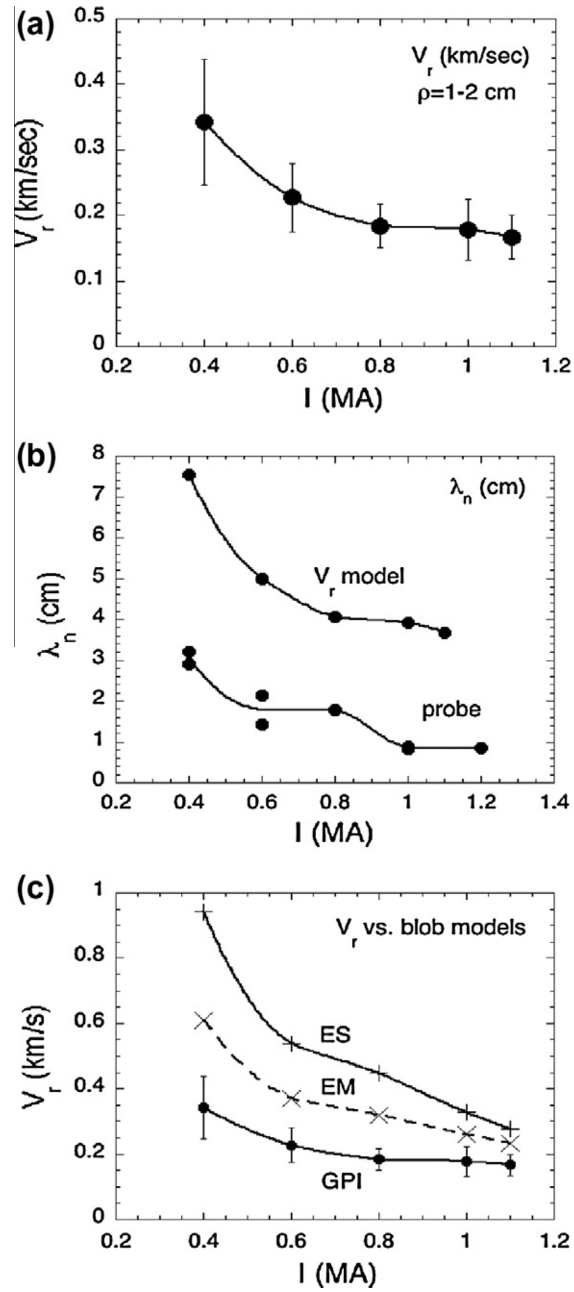

Fig. 2. In part (a) are the average radial velocities from the cross-correlation analysis vs. plasma current. The error bars are the standard deviations of data points such as in Fig. 1, averaged over ρ = 1–2 cm. In part (b) is a comparison of the density SOL widths λ_n inferred from these convective velocities compared with the probe-measured values. In part (c) these velocities are compared with estimates from analytic blob models for electrostatic (ES) and electromagnetic (EM) blobs.

from $V_r \sim$ 0.34 km/s at I = 0.4 MA to $V_r \sim$ 0.17 km/s at I = 1.1 MA. The error bars are the standard deviations of data points such as in Fig. 1, averaged over ρ = 1–2 cm. Movies of the GPI data for shots in this scan can be seen at www.pppl.gov/~szweben under "C-Mod (2009)".

3. Relationship of convective flow to SOL width

The simplest relationship between the radial turbulence velocity calculated near the outer midplane as in Section 2 to the midplane density SOL width λ_n is [7]: $\lambda_n \sim V_r\, \tau_{II,n} \sim V_r\, (L_{II}/V_{II,n})$, where $\tau_{II,n}$ is the parallel transit timescale over which flux surfaces are depleted of density due to particle flow along the field lines to the divertor plate, L_{II} is the parallel distance to the divertor plate, $V_{II,n}$ is the average ion velocity toward the divertor plate, and $n_e(\rho > 0) \propto \exp(-\rho/\lambda_n)$. This model assumes that there is no return of ions along field lines from the divertor to the midplane, and that there is no local ionization source on these flux surfaces near the midplane.

The parallel transit time is not directly measured in this (or any other) experiment, but can be estimated from the theory of classical parallel flow as $V_{II,n} \sim 0.5c_s$, where c_s is the warm ion sound speed [7]. Using $L_{II} \sim 5$ m and T_e–20 eV, which are typical for ρ = 1–2 cm in this experiment, and assuming $T_i = T_e$, the resulting parallel transit time is $\tau_{II,n} \sim 200$ µs. Thus the inferred density SOL width from the model above for the case of Fig. 2 with $V_r \sim 0.2$ km/s is $\lambda_n \sim 4$ cm. This result has at least a factor-of-two uncertainty.

A comparison of the SOL widths estimated in this way with the density SOL e-folding widths measured at ρ = 1–2 using a Langmuir probe in the SOL is shown in Fig. 2b. The result is that the V_r model of above predicts a λ_n which is about a factor of 2–3 larger than the probe results. However, the probe data for these cases are relatively sparse, so the probe results for λ_n are also uncertain by up to a factor-of-two. Thus the level of disagreement shown in Fig. 2b is not too surprising, given these uncertainties.

4. Relationship of SOL width to analytic blob models

Analytic blob models predict radial blob speeds which can be compared with experiments [4]. The simplest blob theory assumes a "sheath-connected" electrostatic (ES) model, and predicts a radial blob speed of: $V_{r,ES} = 2c_s(\rho_s/\delta_b)^2(L_{II}/R)$, where δ_b is the poloidal Gaussian half-width of the blob. This model is reasonable since the normalized SOL collisionality here is only $\nu_e^* \sim 2$. For the case of Fig. 2 at I = 1 MA, R = 67 cm, B = 5.4 T: $c_s \sim 3 \times 10^6$ cm/s, $\rho_s \sim 10^{-2}$ cm, $\delta_b \sim 0.5$ cm, and $L_{II}/R \sim 7.5$, the result is $V_{r,ES} \sim 0.35$ km/s, which is not too far from the measured velocity $V_r \sim 0.2$ km/s of Fig. 1. An alternative blob model is the resistive-X point electromagnetic (EM) regime, where: $V_{r,EM} = q\, c_s^2/V_{Alf}$, where $q \sim (L_{II}/R)$ and V_{Alf} is the Alfven speed. Assuming the measured $n \sim 10^{19}$ m^{-3} for ρ = 1–2 cm, the result is $V_{r,EM} \sim 0.25$ km/s, i.e. also close to the measured value and to the ES result.

Fig. 2c shows a comparison between these model blob speeds and the GPI convective speeds for the current scan discussed above. Given the many uncertainties and oversimplifications in applying these models (e.g. $T_i = 0$), the factor of 2–3 disagreement is not too surprising. It is interesting to note that both models seem to reproduce the inverse current scaling (or B scaling) in the data. However, applying the analytic blob model velocities of Fig. 2c directly to the convective SOL model would overestimate the SOL width by about a factor of 4–9. There are several approximations in the simple blob models which could explain this discrepancy [4]: (a) the blob model velocities should be reduced since the blob propagates on a finite-density background plasma, which was not taken into account, (b) the density and temperature inside a blob may be greater than the averages as measured by the probe, which could reduce the velocity predictions, (c) high speed blobs may contribute mainly to far-SOL and so not be seen in the density e-folding width, and (d) the intermittency of the blob process was not taken into account (see Section 5). Thus the level of disagreement between the probe measurements and this simple model is not too surprising.

5. Blob-tracking estimate of convective velocity and SOL width

To further test the validity of the analytic blob models, an attempt was made to track the motion of individual blobs from frame-to-frame. To do this, the images for each 10 ms time period for each shot were first normalized to their time–average and then smoothed over 3 × 3 pixels, such that a large blob had a relative magnitude of ~2 on this scale. Then the region between the separatrix and the limiter shadow was searched for the largest blob, i.e. maximum pixel in each frame. If the maxima in two successive frames were within ±5 pixels (±0.5 cm) of each other, then the radial velocity for this blob was evaluated. The same procedure was then applied to the next-highest and third-highest maximum in

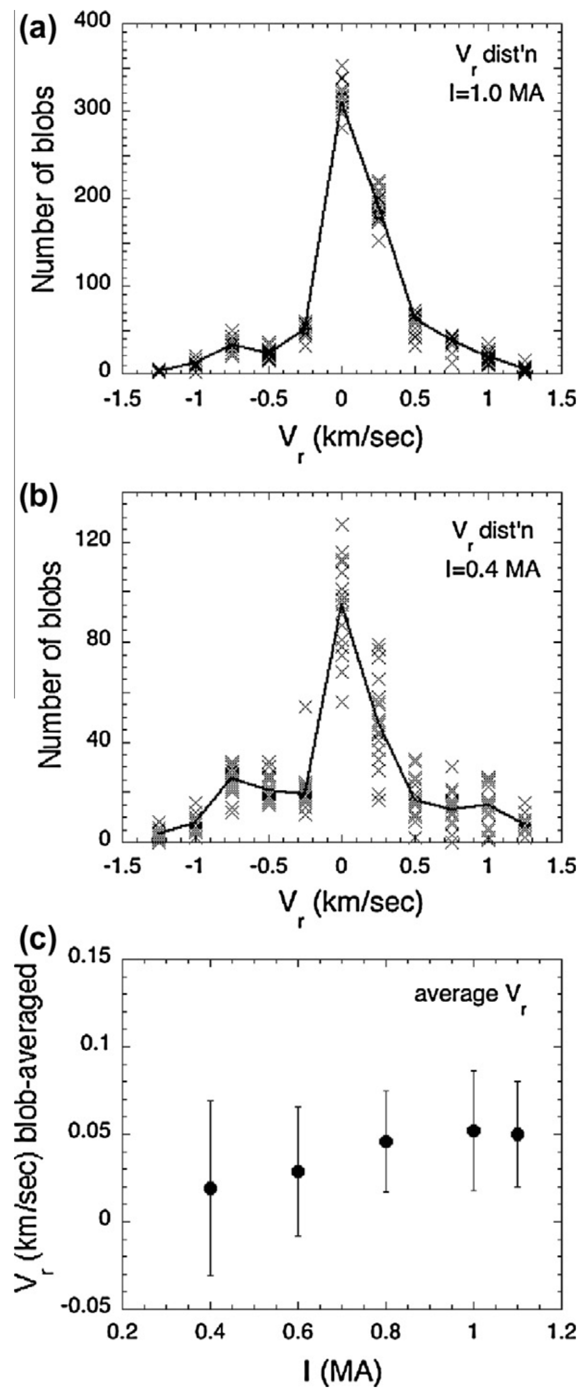

Fig. 3. Analysis of blob motion obtained using the blob-tracking algorithm described in Section 5. In (a) and (b) are the distributions of radial velocity obtained for the ensemble of the largest blobs detected at I = 1 MA and I = 0.4 MA, respectively. In part (c) is the average velocity over all blobs detected as a function of plasma current.

each frame, with the constraint that these maxima were outside ±0.5 cm from each other. This procedure resulted in about one blob track per frame, i.e. ~2500 blobs per 10 ms image sequence.

Fig. 3 shows results from this blob-tracking algorithm for this data set. Parts 3(a) and (b) show the distribution of radial blob velocities for the first maximum for I = 1.0 MA and 0.4 MA, respectively, where the number of blob trajectories during each 10 ms period for each shot is plotted on the vertical axis. There is clearly a positive (outward-going) skewness in the velocity distribution at 1.0 MA, but the distribution at 0.4 MA is nearly in/out symmetrical. Fig. 3c shows the blob-averaged radial velocity as a function of plasma current, weighted by the number of blobs and their relative size, and averaged over all times and shots for all three maxima. At I = 0.8–1.1 MA these averaged velocities are ~3 times *lower* than the convective velocities estimated from cross-correlations in Fig. 2, and at $I \leqslant 0.6$ MA the blob velocities are even lower, i.e. inconsistent with the cross-correlation velocity trend of Fig. 2a. It is important to note that the results of Fig. 3 strongly depend on the exact definition of a blob and the method chosen to track its motion.

A model for the effect of intermittency on SOL particle transport is discussed in [12], in which the effective convective velocity due to blobs is estimated as: $V_{rb} = V_b\,(n_b/n)/C_b$. where V_b is the radial blob velocity, (n_b/n) is the blob density normalized to the background plasma density, and C_b is the ratio of the time between blobs to the lifetime of a blob. The blob-induced convective velocity can be estimated from these blob-tracking results. For the I = 1 MA case, the average blob velocity was $V_b \sim 50$ m/s, and the average ratio (n_b/n) can be taken as the normalized GPI emission level of these blobs, i.e. ~1.5. The C_b term can be approximated by fractional area covered by these blobs, which was $f_b \sim 0.05$; thus roughly $C_b \sim 20$ based on this blob tracking process. An alternate method to estimate C_b is to calculate the packing fraction f_p [13], with a result of $f_p \sim 1$–5% for the region ρ = 1–2 cm; thus if $C_b \sim 1/f_p$ then $C_b \sim 30$. The resulting convective velocity due to blobs is only $V_{rb} \sim 3$ m/s, which is much lower than the convective velocities of Fig. 2a, and very much lower than the analytic blob speeds of Fig. 2c. Thus, according to this analysis, the blobs as defined by this procedure should have little effect on the SOL width in this experiment.

6. Discussion

This paper described attempts to estimate the convective radial transport due to SOL turbulence in Alcator C-Mod. However, it was not possible to accurately explain the observed density SOL width from the convective turbulence velocity, or to explain the observed blob-tracking results based on analytic blob models.

The estimate of the density SOL width from the simple convective model in Section 3 is uncertain due to the assumptions about the parallel connection length and flow speed, and the assumption of purely convective radial flow. However, it is encouraging that the plasma current dependence of λ_n from the V_r model in Fig. 2 agrees with the Langmuir probes in these cases at constant q(a) and SOL parameters, since the connection length and parallel flow should be nearly constant in this scan.

The present blob-tracking algorithm resulted in blob speeds which were much lower than the simplified analytic blob models. In particular, the blob models cannot explain the inward (negative) blob motion seen in these blob-tracking results and previously on C-Mod [11] and NSTX [14]. Thus for a quantitative interpretation of the blob velocity spectrum and the resulting SOL transport it would be preferable to use edge turbulence simulation codes such as ESEL [7], SOLT [9], or BOUT [15].

It is important to note that this analysis of SOL transport is incomplete unless a model for the SOL ionization and particle recycling is included. For example, the effective convective velocity as determined from the particle balance in the SOL of C-Mod ($V_{eff} \sim 10$–100 m/s) was shown to depend on the details of the radial and poloidal variation of the neutral sources [16]. These sources cannot be evaluated from the turbulence alone.

In general, these results point to the need to measure the probability distribution function of plasma velocity in the SOL to determine whether the transport is locally convective or diffusive. Measurements of SOL turbulence should also be directly compared with SOL turbulence simulations [7,9], using common analysis techniques, so that a quantitative understanding of the turbulence-induced SOL width can be obtained.

Acknowledgements

This work was supported by Work supported by US DOE Contracts #DE-AC02-09CH11466 and DE-FC02-99ER54512.

Reference

[1] P. Staib, J. Nucl. Mater. 111–112 (1982) 109.
[2] W. Fundamenski, Power Exhaust in Fusion Plasmas, Cambridge University Press, 2010.
[3] S.J. Zweben, J.A. Boedo, O. Grulke, et al., Plasma Phys. Contr. Fusion 49 (2007) 1.
[4] S.I. Krasheninnikov, D.A. D'Ippolito, J.R. Myra, J. Plasma Phys. 74 (2008) 679; J.R. Myra, D.A. D'Ippolito, D.P. Stotler, et al., Phys. Plasmas 13 (2006) 092509; J.R. Myra, D.A. D'Ippolito, S. I Krasheninnikov, G.Q. Yu, Phys. Plasmas 11 (2004) 4267.
[5] B. LaBombard, J.W. Hughes, N. Smick, et al., Phys. Plasmas 15 (2008) 056106.
[6] J.A. Boedo, D.K. Rudakov, S. Krahseninnikov, Phys. Plasmas 8 (2001) 4826.
[7] W. Fundamenski et al., Nucl. Fusion 47 (2007) 417.
[8] A.Y. Pigarov, S.I. Krasheninnikov, B. LaBombard, T.D. Rognlien, J. Nucl. Mater. 363–365 (2007) 643.
[9] J.R. Myra, D.A. Russell, D.A. D'Ippolito, et al., Paper P3-18 (this conference).
[10] J.L. Terry, S.J. Zweben, O. Grulke, et al., J. Nucl. Mater. 337–339 (2005) 322.
[11] O. Grulke, J.L. Terry, B. LaBombard, S.J. Zweben, Phys. Plasmas 13 (2006) 012306.
[12] S. I Krasheninnikov, A.Y. Pigarov, et al., Phys. Plasmas 16 (2009) 014501.
[13] V. Antoni et al., Eur. Phys. Lett. 54 (2001) 51.
[14] S.J. Zweben, R.J. Maqueda, D.P. Stotler, et al., Nucl. Fusion 44 (2004) 134.
[15] T.D. Rognlien, M.V. Umansky, X.Q. Xu, et al., J. Nucl. Mater. 337 (2005) 327.
[16] B. Lipschultz, D. Whyte, B. LaBombard, Plasmas Phys. Contr. Fusion 47 (2005) 1559.